Apr 26th - May 3rd

Analysis of Stresses in Seismically Induced Shallow Slope Failures

Luis E. Vallejo
Michigan State University, East Lansing, Michigan

Lawrence M. Peszek
Fifield, Palmer and Company, Chicago, Illinois

Proceedings: First International Conference on Recent Advances in Geotechnical Earthquake Engineering and Soil Dynamics, April 26 - May 3, 1981, St. Louis, Missouri

Analysis of Stresses in Seismically Induced Shallow Slope Failures

Luis E. Vallejo
Asst. Prof., Dept. of Civil Engineering, Michigan State University, East Lansing, Michigan

Lawrence M. Peszek
Fifield, Palmer and Company, Chicago, Illinois

SYNOPSIS An analysis of the stresses induced by a combination of static and seismic forces on the failure surface of shallow soil slope instabilities is presented. The geometry of the failures, either shallow planar of finite length or shallow rotational, is taken into consideration in the analysis. The stress induced by a combination of the above forces is found to be greater for the planar than for the rotational ones. Therefore, at limit equilibrium conditions, the former will predominate. Field measurements of the geometry of shallow soil slope failures corroborate the theoretical findings.

INTRODUCTION

Earthquake-induced failures of natural soil slopes can be classified into two major types of mass movement. These are a) deep slip failures and b) shallow slip failures. Skempton and Hutchinson (1969) define the deep failures as those having values for the ratio between the maximum thickness, D , and the length, L , of the slide between 0.15 and 0.33. The shallow failures are defined by Skempton (1953) as those having values of D/L of less than 0.06 . Much material has been published in the geotechnical literature regarding deep failures (Prakash et al., 1969; Sarma, 1973; Vallejo and Edil, 1979). However, shallow failures which have been reported to occur in all seismically active areas of the world (Marimota et al., 1967; Morton, 1971; Stratta and Willie, 1976; Yen and Trotter, 1978) have received little attention, and the need for more information regarding the shallow type of slope failure is recognized in this study.

The shallow soil slope failures can be of two types, translational planar or rotational circular (Skempton and Hutchinson, 1969). The static and seismic induced stresses on their respective failure surfaces, therefore, will be different because of their geometries. A knowledge of the stresses on potential failure surfaces is important when assessing the stability of slopes. The objective of this study is to develop a theoretical analysis of the stresses induced by a combination of static and seismic forces on the failure surfaces of the two types of shallow instabilities in order to determine at limit equilibrium conditions which mode of failure will predominate.

CURRENT METHODS OF ANALYSIS

Current methods of stability analysis of earthquake-induced shallow soil slope failures considers them to behave like either a) an infinite rigid planar translational block (D/L = 0) sliding on a plane parallel to the ground surface and with the assumption that the forces acting at the upper and lower sections of an element of the sliding mass are equal and opposite and hence cancell each other (Fig. 1a)

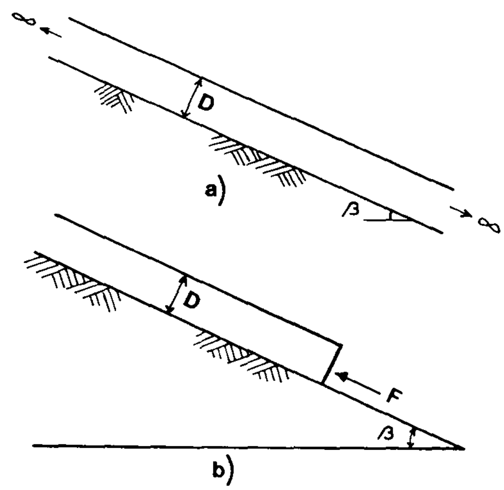

Fig. 1 Geometry of shallow failures considered by current methods of slope stability analysis.

(Finn, 1966), or b) a semi-infinite translational block with the resistant forces against sliding being provided by the shear strength of the soil as well as by a force acting at the toe of the semi-infinite sliding mass (Fig. 1b) (Seed and Goodman, 1964; Yen and Wang, 1977; Yen and Trotter, 1978). Both approaches use the "pseudo-static" method of analysis in which the effect of an earthquake is represented by an inertia force acting at the centroid of the sliding mass.

However, shallow slope instabilities induced by earthquakes have been found by Morton (1971), Yen and Wang (1977) and Yen and Trotter (1978) to have ratios of their maximum thickness, D , and length, L , ranging between 0.01 and 0.03 that will make them neither infinite nor semi-infinite but finite. Also, shallow slope failures can occur, according to Skempton and Hutchinson (1969), in a circular mode as well as in a planar mode.

In the present study the stresses induced by static and seismic forces on the plane of failure of shallow slides will be analyzed assuming first that the instability takes place like a planar slide of finite length, considering therefore the end forces acting on the upper and lower ends of the slide; and second that the instability takes place like a circular rotational slide. A comparison of the values of the resulting stresses will be made in order to assess which mode of failure will predominate. The "pseudo-static" method of analysis is used in the calculations.

PLANAR SLIDE OF FINITE LENGTH

The geometry and forces acting in a finite shallow planar slide are shown in Fig. 2.

on the main block. The passive earth pressure wedge, $A_2B_2C_2$, exerts forces F_p and R_2 on the main block. For the stability analysis of the main block, a knowledge of the values of the forces F_a and F_p is necessary.

<u>The Active Earth Pressure</u>

The active earth pressure, F_a , is calculated from the stability analysis of the wedge $A_1B_1C_1$ of Fig. 2. Each force in the system acting on the wedge is replaced by components in the n_1 direction, perpendicular to the A_1C_1 slip plane, and in the f_1 direction, parallel to CD, the main block's slip plane. A summation of forces in the f_1 direction gives

$$\Big[- F_a + W_1 (\cos \beta \tan \theta_1 + \sin \beta) + a W_1 (\cos \psi - \sin \psi \tan \theta_1) - \frac{T_1}{\cos \theta_1} - R_1 \tan \theta_1\Big] = 0 \qquad [1]$$

In Eq. [1]

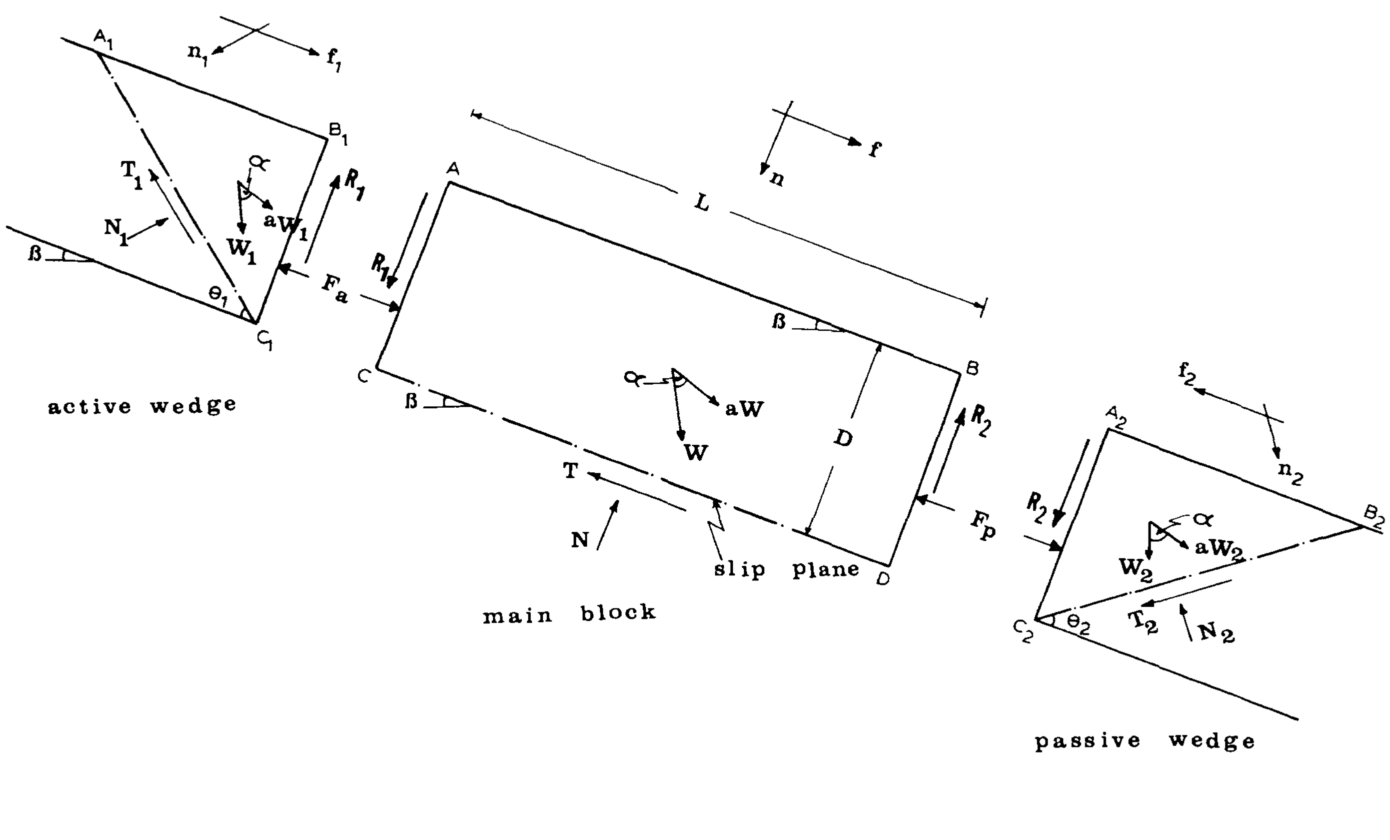

Fig. 2 Geometry and forces acting on a finite shallow planar slide.

The slide is composed of a main sliding block, ABCD , and an active and passive earth wedges located at the two ends of the main block. The active wedge, $A_1B_1C_1$, exerts forces F_a and R_1

$$W_1 = \frac{\gamma D^2}{2 \tan \theta_1} \qquad [2]$$

$$\psi = \alpha + \beta - 90° \quad [3]$$

$$T_1 = \frac{\tau D}{\sin \theta_1} \quad [4]$$

and

$$R_1 = \tau D \quad [5]$$

where W_1 is the weight of the active wedge, β is the inclination of the slope, θ_1 is the strike angle of the active earth pressure wedge, a is the seismic coefficient, α is the angle that the seimic load makes with the vertical direction, T_1 is the shearing force acting on the slip plane of the active earth pressure wedge, R_1 is the shearing force acting on the interface between the active wedge and the main block, and τ is the shear stress.

Replacing Eqs. [2], [4] and [5] into Eq. [1] and after arrangement of terms the following relationship is obtained

$$F_a = \frac{\gamma D^2}{2} [\cos \beta + \frac{\sin \beta}{\tan \theta_1} + \frac{a \cos \psi}{\tan \theta_1} - a \sin \psi] - [\frac{1 + \tan^2 \theta_1}{\tan \theta_1} + \tan \theta_1] \tau D \quad [6]$$

The Passive Earth Pressure

The resultant of the passive earth pressure, F_p , is calculated from the stability analysis of the wedge $A_2B_2C_2$ of Fig. 2. Each force in the system acting on this wedge is replaced by components in the n_2 direction, perpendicular to C_2B_2 slip plane and the f_2 direction which is parallel to CD. In a similar way to how the active earth pressure, F_a , was obtained, the value of the passive earth pressure, F_p , can be calculated from the following relationship

$$F_p = \frac{\gamma D^2}{2} [\cos \beta - \frac{\sin \beta}{\tan \theta_2} - \frac{a \cos \psi}{\tan \theta_2} - a \sin \psi] + [\frac{1 + \tan^2\theta_2}{\tan \theta_2} + \tan \theta_2] \tau D \quad [7]$$

where γ is the unit weight of the soil forming the slope, and θ_2 is the strike angle of the passive earth pressure wedge.

End Wedge Strike Angle Determination

As shown in Eqs. [6] and [7] , F_a and F_p are functions of the angles θ_1 and θ_2 respectively. The values of θ_1 and θ_2 which result in the maximum active and minimum passive earth pressures can be obtained from

$$\frac{d F_a}{d \theta_1} = 0 \quad [8]$$

$$\frac{d F_p}{d \theta_2} = 0 \quad [9]$$

After the differentiation is done the following expression is obtained

$$\theta_1 = \theta_2 = \theta = \text{arc} \tan[\frac{1}{2} - \frac{\gamma D}{4 \tau} (\sin \beta + a \cos \psi)]^{1/2} \quad [10]$$

Main Block Stability Analysis

With the values of F_a and F_p, the stability of the main block, ABCD , can be undertaken (Fig. 2). At limit equilibrium the following expression applies

$$F_a + W \sin \beta + a W \cos \psi - F_p - T = 0 \quad [11]$$

In Eq. [11]

$$W = \gamma L D \quad [12]$$

$$T = \tau L \quad [13]$$

where W is the weight of the main sliding block, T is the shearing force acting on the main slip plane with lenght L.

Replacing the values of F_a , F_p , W ,and T given by Eqs. [6] , [7] , [12] , and [13] into Eq. [11] and simplifying the resulting equation, the following is obtained

$$\tau = \gamma D (\sin \beta + a \cos \psi) (\frac{\tan \theta + r}{\tan \theta + 2 r + 4 r \tan^2 \theta}) \quad [14]$$

where

$$r = \frac{D}{L} \qquad [15]$$

Inserting the value of τ given by Eq.[14] into Eq. [10], the following results

$$\tan\theta = -r + [r^2 + \frac{1}{4}]^{1/2} \qquad [16]$$

If tan θ given by Eq. [16] is inserted into Eq. [14], the following relationship is obtained for the shear stress τ on the failure surface CD (Fig. 2)

$$\tau = \gamma D (\sin\beta + a\cos\psi)(\Delta_p) \qquad [17]$$

where

$$\Delta_p = \frac{1}{1 - 8r^2 + 8r(r^2 + 1/4)^{1/2}} \qquad [18]$$

where Δ_p is the shearing stress coefficient for the case of a planar failure of finite length.

SHALLOW CIRCULAR SLIDE

The geometry and forces acting on a shallow circular slide are shown in Fig. 3 . At limit

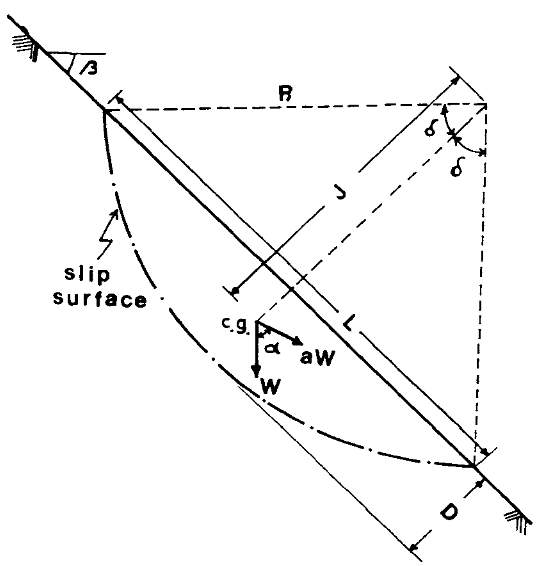

Fig. 3 Geometry and forces acting on a shallow circular slide.

equilibrium conditions the following relationship applies

$$J(W\sin\beta + aW\cos\psi) = 2\tau\delta R^2 \qquad [19]$$

In Eq. [19]

$$J = \frac{2R\sin^3\delta}{3(\delta - \sin\delta\cos\delta)} \qquad [20]$$

and

$$W = \gamma A = \gamma R^2(\delta - \sin\delta\cos\delta) \qquad [21]$$

where J is the distance from the center of gravity of the cross sectional area of the finite circular failure to the center of the failure surface arc, R is the radius of the surface arc, δ is one half of the central angle of the finite circular failure surface arc, and W is the weight of the soil above the circular surface arc.

By substituting the expression of J and W given by Eqs. [20] , and [21] into Eq. [19] the following expression is obtained

$$\tau = \frac{\gamma R}{3\delta}\sin^3\delta[\sin\beta + a\cos\psi] \qquad [22]$$

Also from Fig. 3

$$\sin^3\delta = \frac{L^3}{8R^3} \qquad [23]$$

Substituting Eq. [23] into [22] one obtains

$$\tau = \frac{\gamma L^3[\sin\beta + a\cos\psi]}{24R^2\delta} \qquad [24]$$

From Fig. 3 the following relations can be obtained

$$(R - D)^2 + (\frac{L}{2})^2 = R^2 \qquad [25]$$

and

$$\sin\delta = \frac{L/2}{R} \qquad [26]$$

Eqs. [25] and [26] yield

$$R = \frac{D}{2} + \frac{L^2}{8D} \qquad [27]$$

and

$$\delta = \arcsin\frac{1}{\frac{D}{L} + \frac{1}{4\frac{D}{L}}} \qquad [28]$$

Substituting Eqs. [27] and [28] into [24], and also using Eq. [15], the following final equation, after reduction, is obtained:

$$\tau = \gamma D (\sin \beta + a \cos \psi) (\Delta_c) \qquad [29]$$

where

$$\Delta_c = \frac{1}{\left(6 r^3 + \frac{3}{8r} + 3 r\right) (0.0174) \sin^{-1}\left(\frac{1}{r + \frac{1}{4r}}\right)} \qquad [30]$$

where 0.0174 is a factor to convert degrees to radians, and $\sin^{-1}$ stands for arc sin.

COMPARISON OF SHEAR STRESSES

At limit equilibrium conditions (factor of safety equal to one), the shear stress on the failure surface for the case of a shallow finite planar slide and a shallow circular slide can be obtained from Eqs. [17] and [29] respectively. An analysis of these two equations shows that the only difference between the two is based on the value obtained by the shearing stress coefficients Δ_p and Δ_c which are functions of the ratio r expressed by Eq. [15]. Therefore a comparison of the values of Δ_p and Δ_c for a range of values of r , can answer the question: which mode of failure, planar or circular, will predominate when failure takes place on a soil slope.

A plot of values of Δ_p and Δ_c versus r is shown in Fig. 4. Fig. 4 clearly shows that for

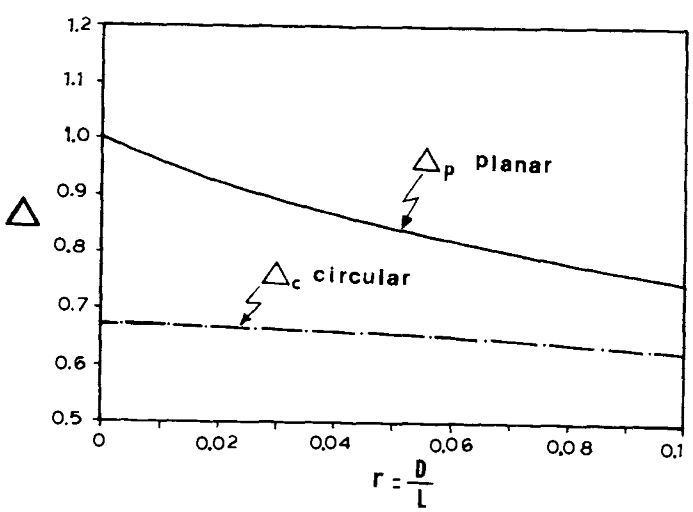

Fig. 4 Relationships between the shearing coefficients Δ_p and Δ_c with respect to the ratio r for the case of shallow soil slope instabilities.

a range of values of r between 0 and 0.1 , the value of the coefficient Δ_p is always greater than the values attained by Δ_c . Therefore, at limit equilibrium conditions, shallow planar slides of finite length will predominate over shallow circular slides. The theoretical findings are corroborated by field measurements conducted by Yen and Wang (1977) and by Yen and Trotter (1978) on the slide geometry of shallow failures induced by a combination of static and seismic loads that took place in the region of Lopez Canyon, California, during the 1971 San Fernando Earthquake.

CONCLUSIONS

A theoretical analysis of stresses induced by a combination of static and seismic forces on the failure surface of shallow soil slope instabilities shows that at limit equilibrium conditions, shallow planar slides of finite length will predominate over shallow rotational slides. Field measurements of reported shallow failures corroborate the theoretical findings.

REFERENCES

Finn, W. D. L. (1966). Earthquake stability of cohesive slopes. Journal of the Soil Mech. and Found. Div., ASCE, Vol. 92, No. SM1, pp. 1-11.

Marimota, R., Nakamura, K., Tsuneishi, Y., Ossaka, J., and Tsunoda, N. (1967). Landslides in the epicentral area of the Matsushiro Earthquake Swarm. Their relation to their Earthquake Fault. Bulletin of the Earthquake Research Institute, Univ. of Tokyo, Vol. 45, pp. 241-263.

Morton, D. M. (1971). Seismically triggered landslides above San Fernado Valley. California Geology, Vol. 24, No. 4-5, pp. 81-82.

Prakash, S., Saran, S., and Purushothamaraj, P. (1969). Seismic analysis of stability of slopes. Proc. of the 7th Int. Conf. on Soil Mech. and Found. Eng., Mexico, Vol. 2, pp. 653-658.

Sarma, S. K. (1973). Stability analysis of embankments and slopes. Geotechnique, Vol. 23, pp. 423-433.

Seed, H. B., and Goodman, R. E. (1964). Earthquake stability of slopes of cohesionless soils. Journal of the Soil Mech. and Found. Div., ASCE, Vol. 90, No. SM6, pp. 3-73.

Skempton, A.W. (1953). Discussion in: Stability problems in road engineering, Edited by R. Glossop and G. C. Wilson. Proc. of the Institution of Civil Engineers, Vol. 2, pp. 219- 280.

Skempton, A. W., and Hutchinson, J. N. (1969). Stability of natural slopes and embankment foundations. Proc. of the 7th Int. Conf. on

Soil Mech. and Found. Eng., Mexico, State of the Art Volume, pp. 291-340.

Stratta, J. L., and Willie, L. A. (1976). Preliminary reconnaissance report on the Italian Earthquake of May 6, 1976. Earthquake Engineering Research Inst. Newsletter, Vol. 10, No. 4, pp. 11-18.

Vallejo, L. E., and Edil T. B., (1979). Design charts for development and stability of evolving slopes. Journal of Civil Engineering Design, Vol. 1, No. 3, pp. 231-252.

Yen, B. C., and Wang, W. L. (1977). Seismically induced shallow hillside slope failures. Proc. 6th World Conf. on Earthquake Eng., Vol. 7, pp. 43-48.

Yen, B. C., and Trotter, J. R. (1978). Shallow slides due to 1971 San Fernado Earthquake. Earthquake Eng. and Soil Dynamics, ASCE Speciality Conference, Pasadena, California, Vol. 2, pp. 1076-1097.

ACKNOWLEDGMENTS

The junior author wishes to express his sincere appreciation to Dr. J. W. Leonard and Professor K. P. Milbradt for providing him with financial assistance which made part of this study possible.